NUCL SCI TECH (2022) 33:45
https://doi.org/10.1007/s41365-022-01028-8

Energy and centrality dependence of light nuclei production in relativistic heavy-ion collisions

Li-Lin Zhu[1] · Bo Wang[1] · Meng Wang[2] · Hua Zheng[2]

Received: 3 November 2021 / Revised: 7 February 2022 / Accepted: 22 February 2022 / Published online: 19 April 2022

Abstract We study the energy and centrality dependence of deuteron and triton (helium-3) production in relativistic heavy-ion collisions at the BNL Relativistic Heavy Ion Collider (RHIC) and CERN Large Hadron Collider (LHC) using the Tsallis distribution, blast-wave (BW) model, and stationary Fokker–Planck (FP) solution. Our study shows that good agreement can be reached between the fitting results from the stationary FP solution and the experimental data for Au + Au collisions from the beam energy scan (BES) program of RHIC at $\sqrt{s_{\mathrm{NN}}}$=7.7, 11.5, 14.5, 19.6, 27, 39, 62.4, and 200 GeV and for Pb + Pb collisions at $\sqrt{s_{\mathrm{NN}}} = 2.76$ TeV. The Tsallis distribution and BW model can reasonably describe the deuteron and triton (helium-3) transverse momentum spectra obtained at RHIC and LHC. A more comprehensive comparison among the three methods suggests that the stationary FP solution is a sensible method, which is able to describe the energy dependence of the light nuclei yield ratio $N_{\mathrm{t}}N_{\mathrm{p}}/N_{\mathrm{d}}^2$ and provide a coherent description of deuteron and triton (helium-3) production for all centralities and various colliding energies at RHIC and LHC.

This work was supported by the National Natural Science Foundation of China (Nos. 11905120 and 11947416).

✉ Hua Zheng
zhengh@snnu.edu.cn

[1] Department of Physics, Sichuan University, Chengdu 610064, China

[2] School of Physics and Information Technology, Shaanxi Normal University, Xi'an 710119, China

Keywords Light nuclei production · Heavy-ion collisions · Tsallis distribution · Blast-wave model · Fokker–Planck solution

1 Introduction

Recently, the production of light nuclei in heavy-ion collisions has been extensively studied at the collision energies available at the Relativistic Heavy Ion Collider (RHIC) and the Large Hadron Collider (LHC) [1–10]. The PHENIX and STAR collaborations at RHIC have reported light nuclei production data for Au + Au collisions at $\sqrt{s_{\mathrm{NN}}} = 7.7 - 200$ GeV [2–4]. The ALICE collaboration has also published data on light nuclei production in p + p collisions at $\sqrt{s_{\mathrm{NN}}} = 0.9$, 2.76, and 7 TeV and in Pb + Pb collisions at $\sqrt{s_{\mathrm{NN}}} = 2.76$ TeV [5, 6]. The energy and centrality dependence of light nuclei production has been a topic of great interest. In addition to the production mechanism, the critical point has also been suggested to be relevant to light nuclei, the study of which is one of the main goals of the beam energy scan (BES) program at RHIC [11–13]. Nevertheless, how and when light nuclei are produced in relativistic heavy-ion collisions are still under debate because of the small binding energies and finite sizes of these nuclei [14–16].

Various scenarios and mechanisms have been proposed to describe the production of light nuclei. Three main approaches are typically used to describe light nuclei production. The first approach is the thermodynamic model [17–21], in which the yields of hadrons and light nuclei are described using a few parameters related to the chemical freeze-out conditions. The production of light nuclei can also be described by the coalescence model, in which it is

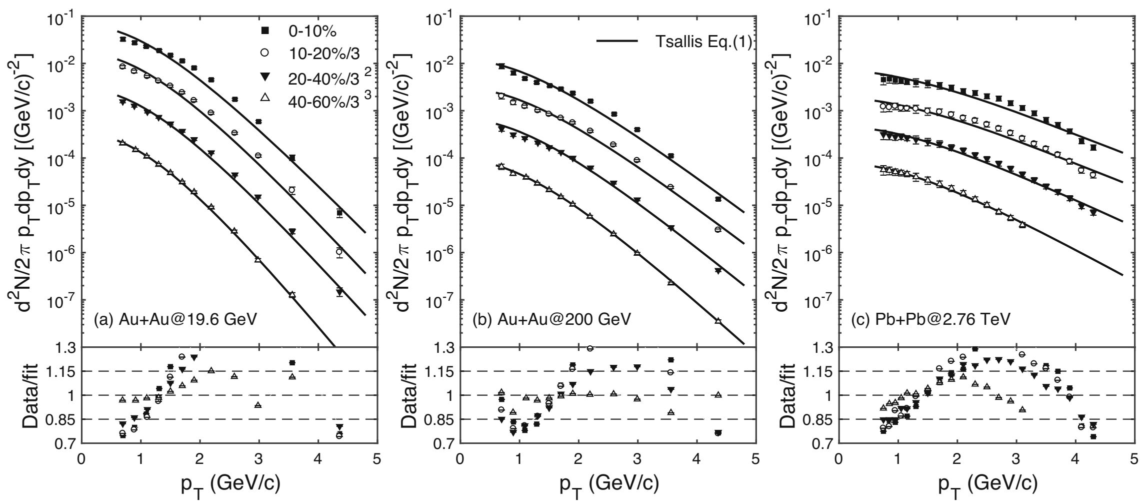

Fig. 1 Fitting results obtained using the Tsallis distribution (Eq. 1) for deuterons in Au + Au collisions at $\sqrt{s_{\mathrm{NN}}} = 19.6$ and 200 GeV and Pb + Pb collisions at $\sqrt{s_{\mathrm{NN}}} = 2.76$ TeV. For better visualization, both the data and curves have been scaled by a constant, as indicated. The data/fit ratios are shown in the bottom panels. The data are obtained from the STAR [3] and ALICE [5] collaborations

assumed that light nuclei are formed through the coalescence of protons and neutrons with similar positions and velocities on the kinetic freeze-out surface [22–30]. The third approach is kinetic theory, in which light nuclei are formed and destroyed during the evolution of the collision system [31–33].

In addition to the above-mentioned approaches, the blast-wave (BW) model has also been widely used by experimental collaborations to describe the transverse momentum (p_{T}) spectra of light nuclei [3–6]. The BW model is motivated by its similarity to the freeze-out configuration of the hydrodynamic model [34]. Despite being a toy model, the spectra of light nuclei produced in Au + Au collisions at $\sqrt{s_{\mathrm{NN}}} = 7.7 \sim 200$ GeV and Pb + Pb collisions at $\sqrt{s_{\mathrm{NN}}} = 2.76$ TeV are impressively well fitted by the BW model [3–5]. The only difference between the two types of collisions is the exponent n in the velocity profile $\beta = \beta_s (\frac{r}{R})^n$, which was set to different values at RHIC and LHC. n was fixed to 1 at RHIC, whereas it was treated as a free parameter at LHC [3, 5].

The Tsallis distribution, which is derived from non-extensive thermodynamics, has been widely applied to describe the final hadron production over a large range of p_{T} in p + p and A + A collisions at RHIC and LHC with great success [35–40]. The stationary Fokker–Planck (FP) solution has also been adopted to describe hadron distributions [39]. To address its inability to fit all the hadron transverse momentum spectra of Pb + Pb collisions that have been identified up to 20 GeV/c, the generalized FP solution was first proposed in Ref. [41]. An excellent fit for the transverse momentum spectra of charged hadrons in Pb + Pb collisions at $\sqrt{s_{\mathrm{NN}}} = 2.76$ TeV and 5.02 TeV and in Xe + Xe collisions at $\sqrt{s_{\mathrm{NN}}} = 5.44$ TeV was obtained [42].

We have been dedicated to the search for a simple universal formula or framework to describe the spectra of particles produced in relativistic heavy-ion collisions [38, 39, 42, 43]. With this as the motivation, it is worth investigating whether the Tsallis distribution, BW model, and stationary FP solution can describe the light nuclei spectra produced at various energies and centralities in relativistic heavy-ion collisions. In this work, we collect experimental data from Au + Au collisions at different collision energies at RHIC and Pb + Pb collisions at LHC and conduct a systematic study of light nuclei production using these three approaches. Based on this analysis, we would like to suggest the optimal approach to describe the energy and centrality dependence of light nuclei production and provide some hints for understanding the mechanism of light nuclei production in relativistic heavy-ion collisions.

The remainder of this paper is organized as follows. In Sect. 2–4, we show our fitting results for the energy and centrality dependence of deuteron and triton (helium-3) production in Au + Au collisions and Pb + Pb collisions obtained using the Tsallis distribution, BW model, and stationary FP solution, respectively. In Sect. 5, a detailed comparison among the three methods and a brief discussion are presented. Finally, a summary is given in Sect. 6.

2 Tsallis distribution

In our previous works [38–40], we demonstrated that several versions of the Tsallis distribution can describe the p_{T} spectra of hadrons produced in both p + p and A + A collisions at RHIC and LHC equally well [38, 39]. The

Tsallis distribution was also adopted by the ALICE collaboration to reproduce the production of deuterons, tritons, helium-3, and their antinuclei in p + p collisions at $\sqrt{s_{\mathrm{NN}}} = 0.9$, 2.76, and 7 TeV [6]. Recently, the energy and centrality dependence of deuteron and triton production in Au + Au collisions was measured at $\sqrt{s_{\mathrm{NN}}} = 7.7$, 11.5, 14.5 19.6, 27, 39, 62.4, and 200 GeV in the STAR experiment of the BES program at RHIC [3, 4]. It is therefore interesting to investigate whether the Tsallis distribution can still describe the production of light nuclei in A + A collisions at RHIC and LHC. In this study, we adopt the following version of the distribution [38–42]:

$$\left(E\frac{\mathrm{d}^3N}{\mathrm{d}p^3}\right)_{|\eta|<a} = A\left(1+\frac{E_{\mathrm{T}}}{nT}\right)^{-n}, \tag{1}$$

where $E_{\mathrm{T}} = \sqrt{p_{\mathrm{T}}^2 + m^2} - m$ is the transverse energy and m is the rest mass of the particle. A, T, and n are free parameters that can be fixed using experimental data. T is the effective temperature and includes the contributions of thermal motion and the flow effect. n is associated with the non-additivity index q of the entropy from the non-extensive statistics for the colliding system.

We analyze the light nuclei production in Au + Au collisions under the BES program at RHIC and in Pb + Pb collisions at LHC using the Tsallis distribution. Similar results are observed for all the energies. In Fig. 1, we show only the fits to the transverse momentum spectra of deuterons using the Tsallis distribution Eq. (1) in Au + Au collisions at $\sqrt{s_{\mathrm{NN}}} = 19.6$ and 200 GeV and in Pb + Pb collisions at $\sqrt{s_{\mathrm{NN}}} = 2.76$ TeV at the four centralities of 0–10%, 10–20%, 20–40%, and 40–60%. The figure also shows the corresponding deuteron distributions from the STAR and ALICE collaborations [3, 5]. It is observed that the Tsallis distribution fits the experimental data for 40–60% centrality at the three energies very well. This is not surprising because the hadron spectra in p + p collisions, which create a similar environment to that of peripheral collisions in A + A collisions, are well fitted by the Tsallis distribution shown in Refs. [6, 38]. For central and less central collisions, the Tsallis distribution underestimates the experimentally measured deuteron transverse momentum spectra in the intermediate p_{T} region at the three collision energies, as shown in Fig. 1. This underestimation relative to peripheral collisions is attributed to medium and/or dynamical effects in the central and less central collisions. Furthermore, to show the agreement between the data and the Tsallis distribution on a linear scale, the deviations of the spectra from the Tsallis distribution are presented as the data/fit ratio in the bottom panels of Fig. 1. The maximum deviation clearly exceeds 30% for central collisions. It should also be noted that the fitting p_{T} range is not large. This indicates that the Tsallis distribution is suboptimal for deuteron production.

We also apply the Tsallis distribution to the transverse momentum spectra of tritons. The fitting results for the triton distributions in Au + Au collisions at $\sqrt{s_{\mathrm{NN}}} = 19.6$ and 200 GeV from central to peripheral collisions are shown in Fig. 2a, b. The situation is somewhat different for Pb + Pb collisions at $\sqrt{s_{\mathrm{NN}}} = 2.76$ TeV. Helium-3 is investigated instead of triton in Fig. 2c because the triton data are not available. It can be seen from the triton data/fit ratios in the bottom panels of Fig. 2a, b that the relative discrepancies are similar to those for deuteron discussed above. In comparison, the worst fitting results are obtained for helium-3 in Pb + Pb collisions at $\sqrt{s_{\mathrm{NN}}} = 2.76$ TeV. This may be related to the fitting p_{T} range, which is almost twice as large as that for tritons in Au + Au collisions.

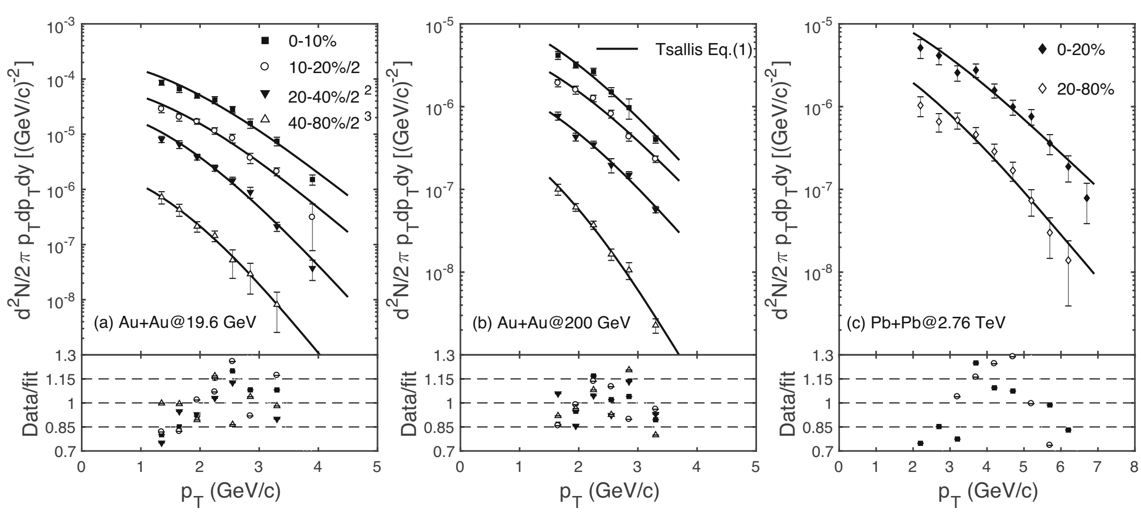

Fig. 2 Same as Fig. 1 for tritons in Au + Au collisions at $\sqrt{s_{\mathrm{NN}}} = 19.6$ and 200 GeV [4] and helium-3 in Pb + Pb collisions at $\sqrt{s_{\mathrm{NN}}} = 2.76$ TeV [5]

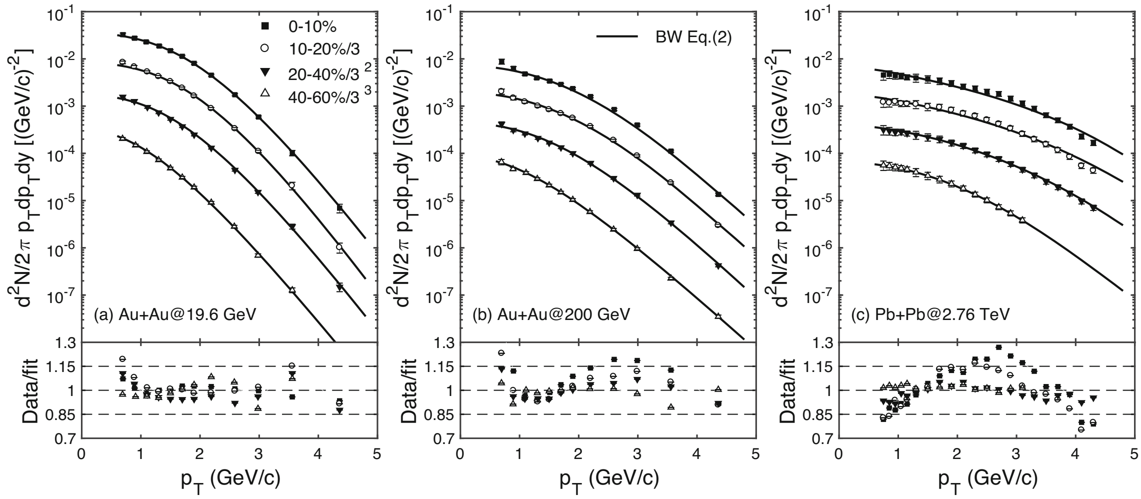

Fig. 3 Fitting results obtained using the BW model (Eq. 2) for deuterons in Au + Au collisions at $\sqrt{s_{\mathrm{NN}}} = 19.6$ and 200 GeV and Pb + Pb collisions at $\sqrt{s_{\mathrm{NN}}} = 2.76$ TeV. For better visualization, both the data and curves have been scaled by a constant, as indicated. The data/fit ratios are shown in the bottom panels. The data are obtained from the STAR [3] and ALICE [5] collaborations

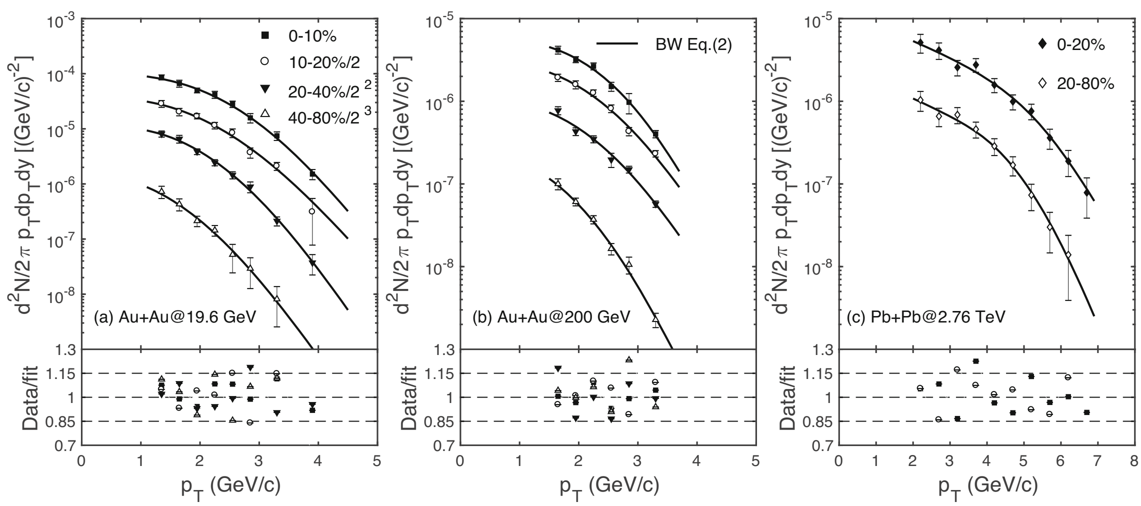

Fig. 4 Same as Fig. 3 for tritons in Au + Au collisions at $\sqrt{s_{\mathrm{NN}}} = 19.6$ and 200 GeV [4] and helium-3 in Pb + Pb collisions at $\sqrt{s_{\mathrm{NN}}} = 2.76$ TeV [5]

3 The blast-wave model

Besides the Tsallis distribution, the BW model is also commonly adopted by experimental collaborations [3–5]. This model describes particle production under the assumption that the particles are thermally emitted from an expanding source. The functional form of this model is given by

$$\frac{1}{p_{\mathrm{T}}}\frac{\mathrm{d}^2N}{\mathrm{d}p_{\mathrm{T}}} \propto \int_0^R r\mathrm{d}r m_{\mathrm{T}} I_0\left(\frac{p_{\mathrm{T}}\sinh\rho}{T}\right)K_1\left(\frac{m_{\mathrm{T}}\cosh\rho}{T}\right), \tag{2}$$

where $m_{\mathrm{T}} = \sqrt{p_{\mathrm{T}}^2 + m^2}$ is the transverse mass, I_0 and K_1 are the modified Bessel functions, and T is the kinetic freeze-out temperature. The velocity profile, ρ, is given by

$$\rho = \tanh^{-1}[\beta_{\mathrm{s}}(r/R)^n], \tag{3}$$

where β_{s} is the transverse expansion velocity at the surface, r the radial distance from the center of the thermal source in the transverse plane, R the radius of the thermal source, and n the exponent of the velocity profile. Experimentally, n was fixed at 1 for the (anti)deuteron distributions in Au + Au collisions at $\sqrt{s_{\mathrm{NN}}} = 7.7$–200 GeV at RHIC [3], whereas for Pb + Pb collisions at $\sqrt{s_{\mathrm{NN}}} = 2.76$ TeV [5], n was treated as a free parameter to obtain a better fit. The different treatments of the parameter n for deuteron production at RHIC and LHC reflect the different dynamical evolution behaviors of the fire balls produced in heavy-ion collisions. In this work, we fix the parameter n to 1 for both Au + Au and Pb + Pb collisions to check the universality of the BW model. There are therefore three free parameters comprising T, β_s, and the normalization factor.

Similar to the Tsallis distribution, we present only the fitting results obtained using Eq. (2) for Au + Au collisions at $\sqrt{s_{\mathrm{NN}}} = 19.6$ and 200 GeV and for Pb + Pb collisions at $\sqrt{s_{\mathrm{NN}}} = 2.76$ TeV. Figures 3 and 4 show that better fitting results are obtained compared to those obtained using Eq. (1), especially for tritons. For the deuterons produced in Au + Au collisions at $\sqrt{s_{\mathrm{NN}}} = 19.6$ and 200 GeV shown in Fig. 3, the discrepancies of the data/fit ratios for all centralities are mostly less than 15%, while those for the fitting results in the intermediate p_{T} region for central Pb + Pb collisions at $\sqrt{s_{\mathrm{NN}}} = 2.76$ TeV reach up to 30% because the parameter n is fixed to 1. Recent studies [24, 26] have shown that when the phase-space distributions of protons and neutrons generated by a sophisticated hydrodynamic model, the iEBE-MUSIC hybrid model [44], are used in the coalescence model, light nuclei production in Au + Au collisions at $\sqrt{s_{\mathrm{NN}}} = 200$ GeV can be reproduced well, but the deuteron yield is slightly overestimated and the yield of helium-3 is underestimated by a factor of approximately 2 for central Pb + Pb collisions at $\sqrt{s_{\mathrm{NN}}} = 2.76$ TeV [24]. These results suggest that the dynamical evolution of the medium in Au + Au collisions differs slightly from that in Pb + Pb collisions. This picture is consistent with the different values of n chosen for the BW model by the RHIC and LHC collaborations. Figure 4 shows that the triton distributions in Au + Au collisions at $\sqrt{s_{\mathrm{NN}}} = 19.6$ and 200 GeV and helium-3 distributions in Pb + Pb collisions at $\sqrt{s_{\mathrm{NN}}} = 2.76$ TeV are well reproduced by Eq. (2).

4 The Fokker–Planck solution

Based on the results in Sects. 2 and 3, it can be seen that neither the Tsallis distribution nor the BW model is the optimal universal formula for describing the transverse momentum spectra of light nuclei at RHIC and LHC. Considering the solution of the FP equation to study the rapidity spectra of net proton production at RHIC [45] and the good performance of the generalized FP solution in describing the identified hadron spectra produced in Pb + Pb collisions at $\sqrt{s_{\mathrm{NN}}} = 2.76$ and 5.02 TeV and in Xe+Xe collisions at $\sqrt{s_{\mathrm{NN}}} = 5.44$ TeV across a very large p_{T} range in our previous works [41, 42], we propose the stationary solution of the FP equation,

$$E\frac{\mathrm{d}^3N}{\mathrm{d}p^3} = A\frac{e^{-\frac{b}{T}\arctan\frac{E_{\mathrm{T}}}{b}}}{\left[1+\left(\frac{E_{\mathrm{T}}}{b}\right)^2\right]^c}, \tag{4}$$

as the universal formula for the light nuclei spectra at RHIC and LHC. In Eq. (4), A, b, c, and T are free parameters.

Figures 5 and 6, respectively, show the experimental data for the transverse momentum spectra of deuterons and tritons in Au + Au collisions at $\sqrt{s_{\mathrm{NN}}} = 7.7$, 11.5, 14.5, 19.6, 27, 39, 62.4, and 200 GeV and the four centralities obtained under the BES program. The solid lines represent the fitting results from Eq. (4) for each distribution. The fitting for deuterons and tritons in Au + Au collisions at RHIC obtained using Eq. (4) is quite good for a wide range of collision energies. The results in Figs. 5 and 6 are indeed encouraging. Therefore, we repeat the fitting process for deuterons and helium-3 produced in Pb + Pb collisions at $\sqrt{s_{\mathrm{NN}}} = 2.76$ TeV at LHC and obtain excellent results, especially for deuterons, as shown in Fig. 7. The ratios shown in the bottom panel of Fig. 7a are almost equal to 1 across the whole p_{T} region for the four centralities. The discrepancy between the data and fit in Fig. 7b is approximately 15% and can be partially attributed to the low statistics of the helium-3 data. Therefore, based on the results shown in Figs. 5, 6 and 7, we conclude that the stationary FP solution can describe light nuclei production in A + A collisions at different colliding energies and centralities well.

5 Discussion

From the above results, we have learned that the three different methods, i.e., the Tsallis distribution, BW model, and stationary FP solution, can describe the experimental data in general. To explicitly compare the agreement of the fitting results obtained using the three approaches with the experimental data, we define the relative discrepancy as the ratio

$$R = \frac{\mathrm{Data}-\mathrm{Fitted}}{\mathrm{Data}}. \tag{5}$$

This ratio can be used to determine which of the three methods is the optimal one for describing the transverse momentum distributions of light nuclei produced at RHIC and LHC.

Figure 8 shows the values of the ratio R obtained using Eqs. (1), (2) and (4) for deuterons (solid symbols) and tritons/helium-3 (empty symbols) as functions of p_{T} on a linear scale for central collisions. The largest discrepancy for deutrons occurs for Au + Au collisions at $\sqrt{s_{\mathrm{NN}}} = 19.6$ and 200 GeV while that for tritons/helium-3 occurs for

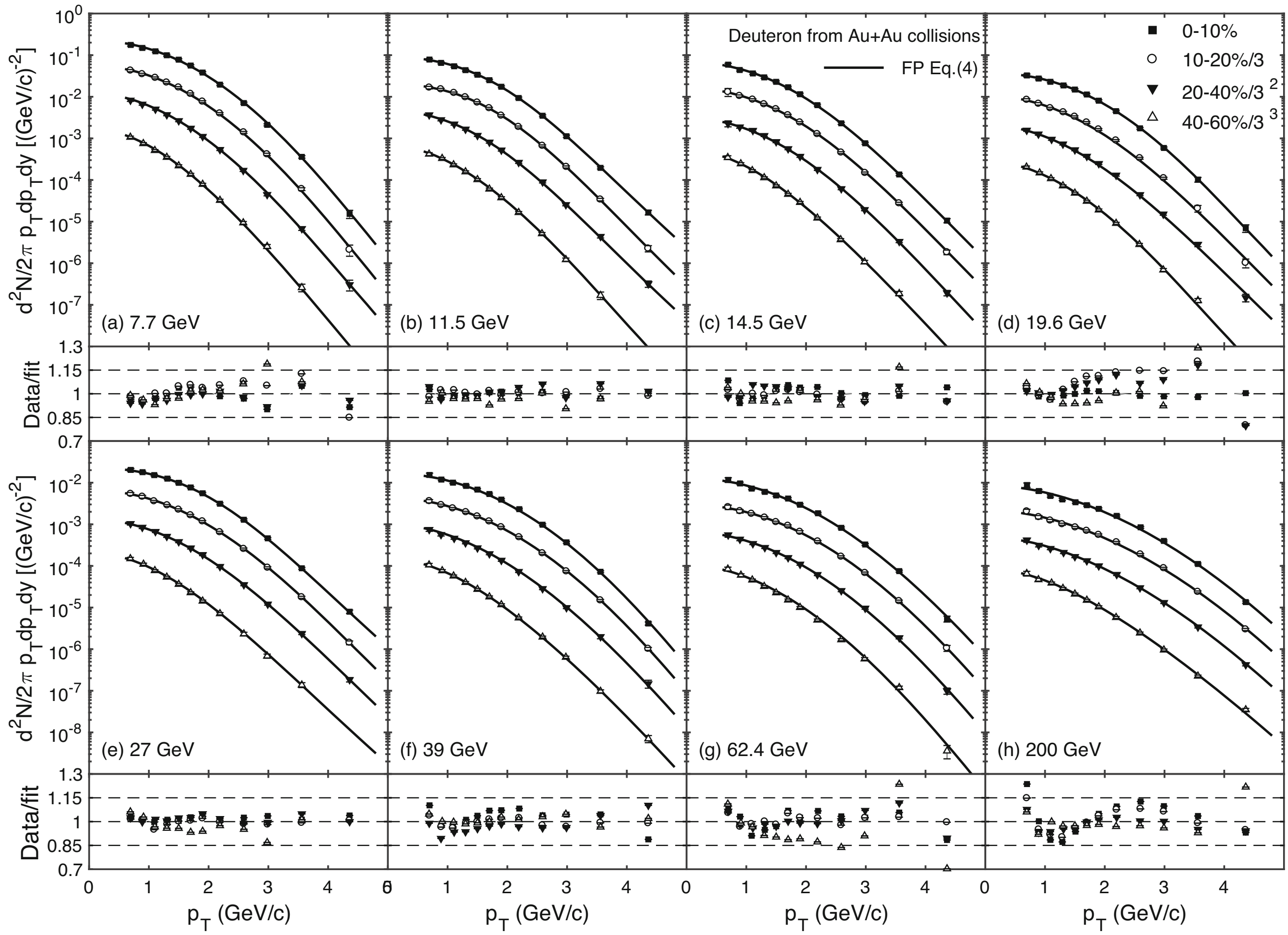

Fig. 5 Fitting results obtained using the stationary FP solution (Eq. 4) for deuterons in Au + Au collisions at $\sqrt{s_{\mathrm{NN}}} = 7.7$–200 GeV. For better visualization, both the data and curves have been scaled by a constant, as indicated. The data/fit ratios are shown in the bottom panels. The data are obtained from the STAR collaboration [3]

Pb + Pb collisions at $\sqrt{s_{\mathrm{NN}}} = 2.76$ TeV. The experimental data for 0–10% centrality were used for deuterons and tritons [3, 4], while the 0–20% centrality data were used for helium-3 [5]. From Fig. 8a, it can be seen that the maximum derivation for deuterons calculated using Tsallis distribution Eq. (1) (solid black squares) is approximately 40% for Au + Au collisions at $\sqrt{s_{\mathrm{NN}}} = 19.6$ GeV. The ratios for the BW model in Eq. (2) (solid red circles) for Au + Au collisions at $\sqrt{s_{\mathrm{NN}}} = 19.6$ GeV shown in Fig. 8a are less than 10%, while the ratios for the two higher energies shown in Fig. 8b, c oscillate between -0.3 and 0.3. These results show that the Tsallis distribution and BW model can only comparatively describe the transverse momentum spectra of deuterons produced at RHIC and LHC. The relative discrepancies for the stationary FP solution Eq. (4) (solid blue triangles), which are in the range between -0.1 and 0.1 for the three energies shown in Fig. 8, are significantly smaller than those for the Tsallis distribution and BW model. These results indicate that among the three methods, the stationary FP solution is the optimal one for describing the transverse momentum spectra of deuterons produced at RHIC and LHC.

To perform a comprehensive evaluation, it is also necessary to check the relative discrepancies for tritons, which are shown with empty symbols in Fig. 8. The ratios for tritons obtained using Eqs. (1), (2), and (4) are generally smaller than those for deuterons at the three collision energies. In more detail, the relative discrepancies for Eq. (1) (empty black squares) are generally larger than those for Eq. (2) (empty red circles) and Eq. (4) (empty blue triangles). The results demonstrate that both the BW model and stationary FP solution are better than the Tsallis distribution for reproducing the triton spectra at various collision energies.

Based on the above-detailed comparisons, we can conclude that the stationary FP solution is the optimal method for describing the deuteron and triton (helium-3) transverse momentum spectra of central to peripheral collisions at

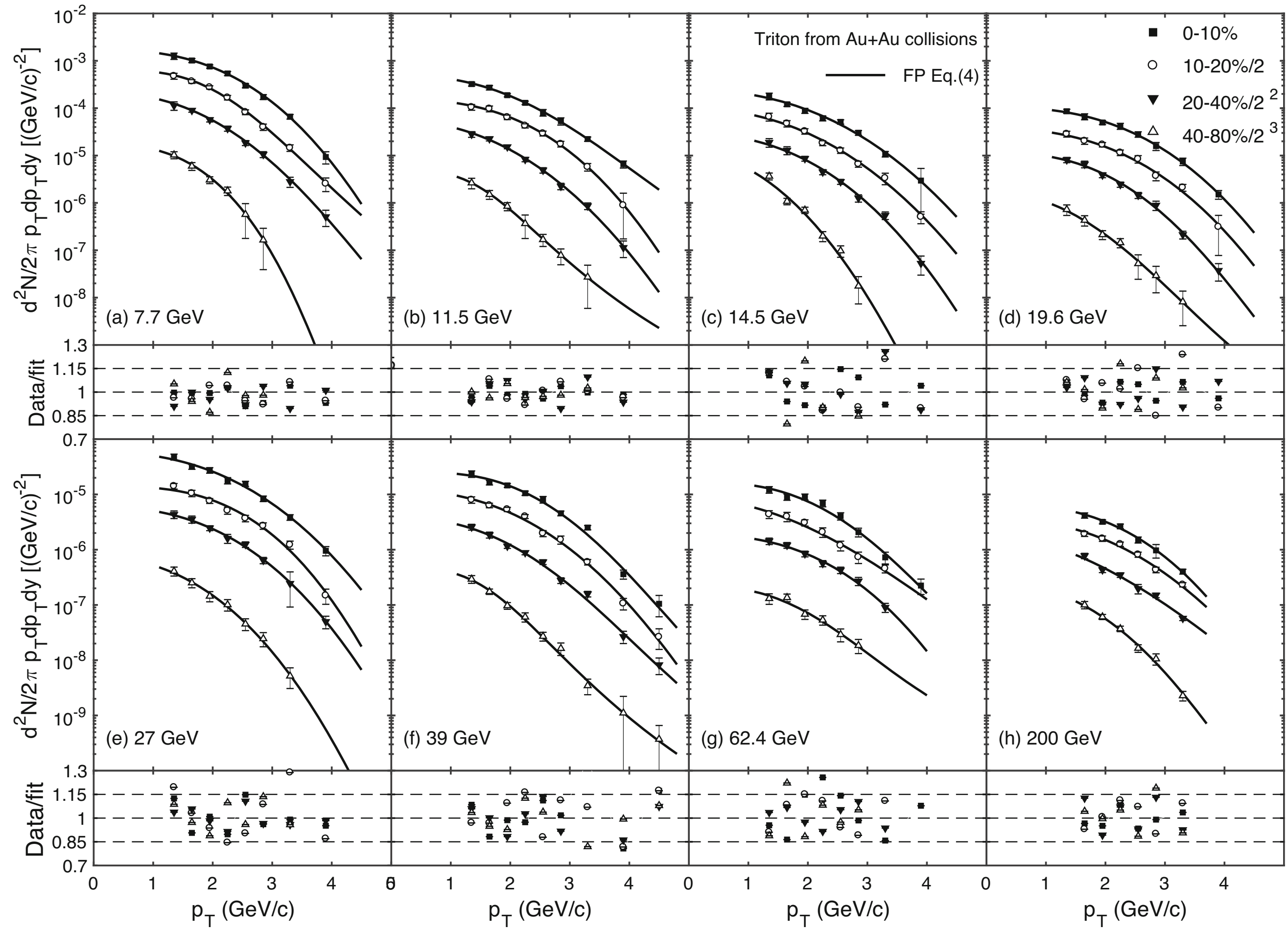

Fig. 6 Same as Fig. 5 for tritons with experimental data from the STAR collaboration [4]

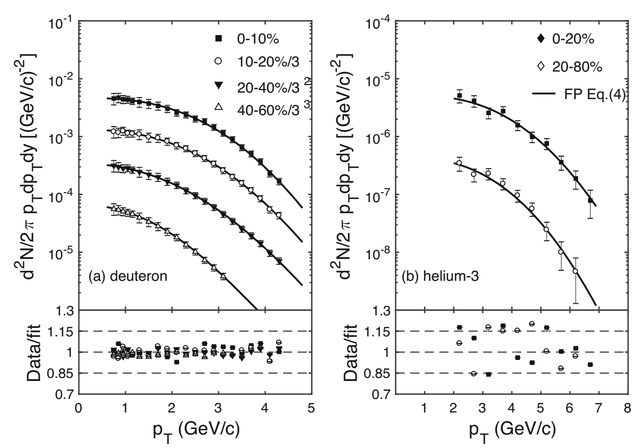

Fig. 7 Fitting results obtained using the stationary FP solution (Eq. 4) for deuterons and helium-3 produced in Pb + Pb collisions at $\sqrt{s_{\mathrm{NN}}} = 2.76$ TeV. For better visualization, both the data and curves have been scaled by a constant, as indicated. The data/fit ratios are shown at the bottom panels. The data are obtained from the ALICE collaboration [5]

RHIC and LHC across a wide range of collision energies from $\sqrt{s_{\mathrm{NN}}} = 7.7$ GeV to 2.76 TeV.

Figure 9 shows the energy dependence of the light nuclei yield ratio $N_{\mathrm{t}}N_{\mathrm{p}}/N_{\mathrm{d}}^2$ at 0-10% centrality for Au + Au collisions. It has been suggested that this ratio can be used to probe the QCD phase diagram [12, 14]. The red solid circles are the preliminary results for BES energies obtained by the STAR collaboration [4]. The yield ratio exhibits a non-monotonic energy dependence. The yield ratios obtained using the Tsallis distribution, BW model, and the stationary FP solution are represented by the lines with blue empty triangles, magenta empty diamonds, and black full squares, respectively. It is obvious that the black line (the stationary FP solution) best reproduces the experimental data, which is consistent with the conclusion above. Our results indicate that transport or hydrodynamic models should reproduce the transverse momentum spectra of light nuclei with a high level of accuracy to quantitatively reproduce the $N_{\mathrm{t}}N_{\mathrm{p}}/N_{\mathrm{d}}^2$ ratio.

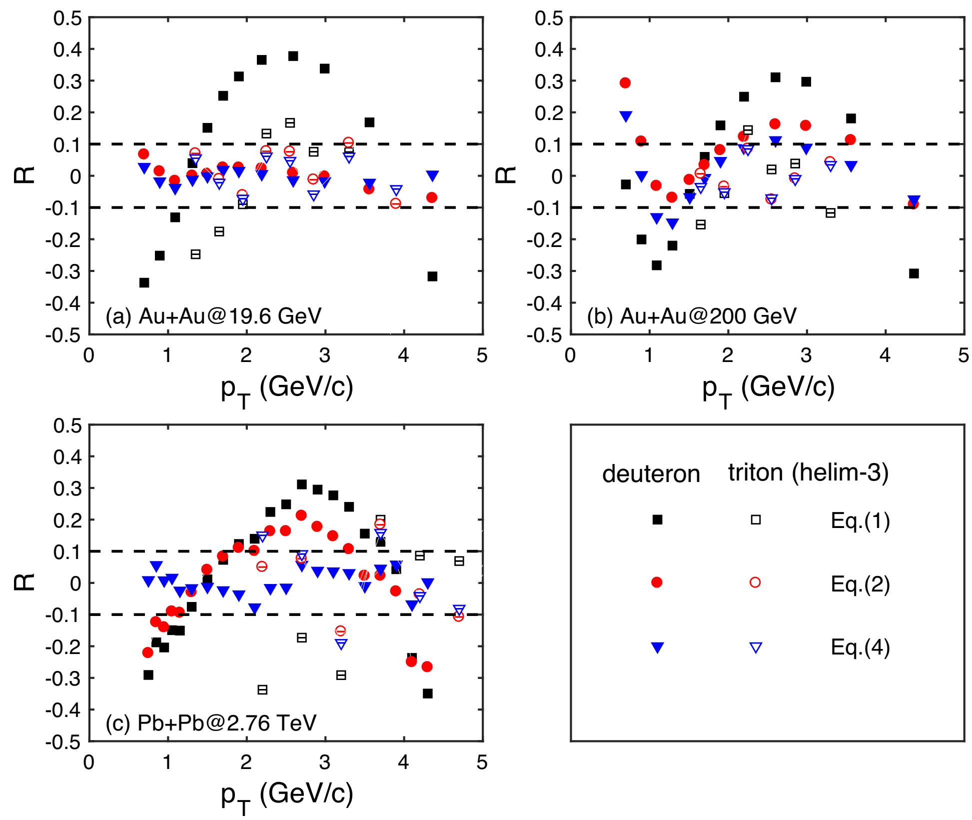

Fig. 8 (Color online) Relative discrepancies of Eqs. (1), (2), and (4) for the p_T spectra of deuterons and tritons (helium-3) in Au + Au central collisions at $\sqrt{s_{NN}} = 19.6$ and 200 GeV and in Pb + Pb collisions at $\sqrt{s_{NN}} = 2.76$ TeV based on the deuteron and triton data for 0–10% centrality [3, 4] and helium-3 data for 0–20% centrality. [5]

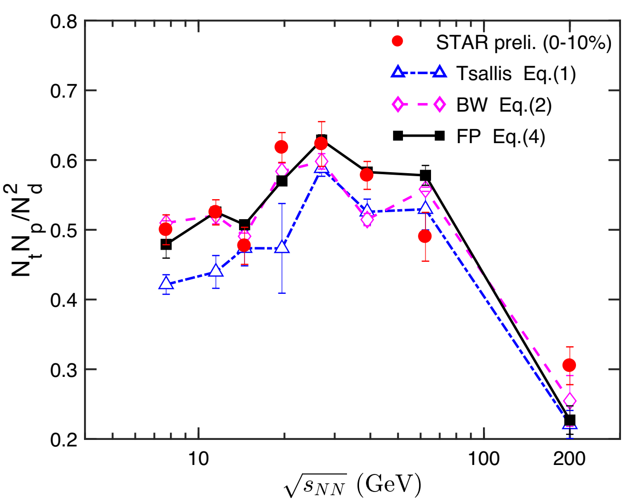

Fig. 9 (Color online) Light nuclei yield ratio $N_t N_p / N_d^2$ as a function of the collision energy $\sqrt{s_{NN}}$ for central Au + Au collisions. The results for the Tsallis distribution, BW model, and stationary FP solution are denoted by their respective lines. The preliminary experimental data (red solid circles) were obtained from Ref. [4]

6 Summary

In this paper, we presented a detailed study of the Tsallis distribution, BW model, and stationary FP solution in which fitting was performed on the transverse momentum spectra of light nuclei produced in Au + Au collisions under the BES program at $\sqrt{s_{NN}}$ =7.7, 11.5, 14.5, 19.6, 27, 39, 62.4, and 200 GeV and in Pb + Pb collisions at $\sqrt{s_{NN}} = 2.76$ TeV. In general, these three approaches can be used to describe the transverse momentum spectra of deuterons and tritons (helium-3) at RHIC and LHC because the maximum relative discrepancy is approximately 40%. However, based on the detailed comparison of the three methods, which included the energy dependence of the light nuclei yield ratio $N_t N_p / N_d^2$, it is clear that the stationary FP solution is the optimal approach for a universal description of the energy and centrality dependence of light nuclei production at RHIC and LHC. We expect our conclusion to be supported by light nuclei produced in Pb + Pb collisions at $\sqrt{s_{NN}} = 5.02$ TeV and in Xe+Xe collisions at $\sqrt{s_{NN}} = 5.44$ TeV in the near future.

Author's contribution All authors contributed to the study conception and design. Material preparation, data collection and analysis were performed by Li-Lin Zhu, Bo Wang, Meng Wang, and Hua Zheng. The first draft of the manuscript was written by Li-Lin Zhu and Hua Zheng and all authors commented on previous versions of the manuscript. All authors read and approved the final manuscript.

References

1. T. Anticic, B. Baatar, J. Bartke et al., Production of deuterium, tritium, and He3 in central Pb + Pb collisions at 20A, 30A, 40A, 80A, and 158A GeV at the CERN Super Proton Synchrotron. Phys. Rev. C **94**, 044906 (2016). https://doi.org/10.1103/PhysRevC.94.044906
2. S.S. Adler, S. Afanasiev, C. Aidala et al., Deuteron and anti-deuteron production in Au + Au collisions at $\sqrt{s_{NN}}$ = 200 GeV. Phys. Rev. Lett. **94**, 122302 (2005). https://doi.org/10.1103/PhysRevLett.94.122302
3. J. Adam, L. Adamczyk, J.R. Adams et al., Beam energy dependence of (anti-)deuteron production in Au + Au collisions at the BNL Relativistic Heavy Ion Collider. Phys. Rev. C **99**, 064905 (2019). https://doi.org/10.1103/PhysRevC.99.064905
4. D. Zhang, Light nuclei (d, t) production in Au + Au collisions at $\sqrt{s_{\rm NN}}$ = 7.7–200 GeV. Nucl. Phys. A **1005**, 121825 (2021). https://doi.org/10.1016/j.nuclphysa.2020.121825
5. J. Adam, D. Adamová, M.M. Aggarwal et al., Production of light nuclei and anti-nuclei in pp and Pb–Pb collisions at energies available at the CERN Large Hadron Collider. Phys. Rev. C **93**, 024917 (2016). https://doi.org/10.1103/PhysRevC.93.024917
6. S. Acharya, J. Adam, D. Adamová et al., Production of deuterons, tritons, ^{3}He nuclei and their antinuclei in pp collisions at $\sqrt{s}$ = 0.9, 2.76 and 7 TeV. Phys. Rev. C **97**, 024615 (2018). https://doi.org/10.1103/PhysRevC.97.024615
7. J. Adam et al., $^3_\Lambda$H and $^3_{\bar\Lambda}\overline{\rm H}$ production in Pb–Pb collisions at $\sqrt{s_{\rm NN}}$ = 2.76 TeV. Phys. Lett. B **754**, 360 (2016). https://doi.org/10.1016/j.physletb.2016.01.040
8. S. Acharya, D. Adamová, J. Adolfsson et al., Measurement of deuteron spectra and elliptic flow in Pb–Pb collisions at $\sqrt{s_{\rm NN}}$ = 2.76 TeV at the LHC. Eur. Phys. J. C **77**, 658 (2017). https://doi.org/10.1140/epjc/s10052-017-5222-x
9. J. Chen, D. Keane, Y.G. Ma et al., Antinuclei in heavy-ion collisions. Phys. Rep. **760**, 1–39 (2018). https://doi.org/10.1016/j.physrep.2018.07.002
10. P. Liu, J. H. Chen, Y. G. Ma et al., Production of light nuclei and hypernuclei at High Intensity Accelerator Facility energy region. Nucl. Sci. Tech. **28**, 55 (2017). https://doi.org/10.1007/s41365-017-0207-x. Erratum to: Production of light nuclei and hypernuclei at High Intensity Accelerator Facility energy region. Nucl. Sci. Tech. **28**, 89 (2017). https://doi.org/10.1007/s41365-017-0224-9
11. X. Luo, N. Xu, Search for the QCD critical point with fluctuations of conserved quantities in relativistic heavy-ion collisions at RHIC: An overview. Nucl. Sci. Tech. **28**, 112 (2017). https://doi.org/10.1007/s41365-017-0257-0
12. K.J. Sun, L.W. Chen, C.M. Ko et al., Probing QCD critical fluctuations from light nuclei production in relativistic heavy-ion collisions. Phys. Lett. B **774**, 103 (2017). https://doi.org/10.1016/j.physletb.2017.09.056
13. E. Shuryak, J.M. Torres-Rincon, Light-nuclei production and search for the QCD critical point. Eur. Phys. J. A **56**, 241 (2020). https://doi.org/10.1140/epja/s10050-020-00244-3
14. K.J. Sun, L.W. Chen, C.M. Ko et al., Light nuclei production as a probe of the QCD phase diagram. Phys. Lett. B **781**, 499 (2018). https://doi.org/10.1016/j.physletb.2018.04.035
15. S. Mrowczynski, Production of light nuclei in the thermal and coalescence models. Acta Phys. Polon. B **48**, 707 (2017). https://doi.org/10.5506/APhysPolB.48.707
16. X. Xu, R. Rapp, Production of light nuclei at thermal freezeout in ultrarelativistic heavy-ion collisions. Eur. Phys. J. A **55**, 68 (2019). https://doi.org/10.1140/epja/i2019-12757-7
17. A. Andronic, P. Braun-Munzinger, J. Stachel et al., Production of light nuclei, hypernuclei and their antiparticles in relativistic nuclear collisions. Phys. Lett. B **697**, 203 (2011). https://doi.org/10.1016/j.physletb.2011.01.053
18. A. Andronic, P. Braun-Munzinger, K. Redlich et al., Decoding the phase structure of QCD via particle production at high energy. Nature **561**, 321 (2018). https://doi.org/10.1038/s41586-018-0491-6
19. V. Vovchenko, K. Gallmeister, J. Schaffner-Bielich et al., Nucleosynthesis in heavy-ion collisions at the LHC via the Saha equation. Phys. Lett. B **800**, 135131 (2020). https://doi.org/10.1016/j.physletb.2019.135131
20. J. Cleymans, S. Kabana, I. Kraus et al., Antimatter production in proton–proton and heavy-ion collisions at ultrarelativistic energies. Phys. Rev. C **84**, 054916 (2011). https://doi.org/10.1103/PhysRevC.84.054916
21. A. Andronic, P. Braun-Munzinger, K. Redlich et al., The thermal model on the verge of the ultimate test: particle production in Pb–Pb collisions at the LHC. J. Phys. G **38**, 124081 (2011). https://doi.org/10.1088/0954-3899/38/12/124081
22. K.J. Sun, L.W. Chen, Production of antimatter ^{5,6}Li nuclei in central Au+Au collisions at $\sqrt{s_{NN}}$ = 200 GeV. Phys. Lett. B **751**, 272 (2015). https://doi.org/10.1016/j.physletb.2015.10.056
23. L. Zhu, C.M. Ko, X. Yin, Light (anti-)nuclei production and flow in relativistic heavy-ion collisions. Phys. Rev. C **92**, 064911 (2015). https://doi.org/10.1103/PhysRevC.92.064911
24. W. Zhao, L. Zhu, H. Zheng et al., Spectra and flow of light nuclei in relativistic heavy ion collisions at energies available at the BNL Relativistic Heavy Ion Collider and at the CERN Large Hadron Collider. Phys. Rev. C **98**, 054905 (2018). https://doi.org/10.1103/PhysRevC.98.054905
25. L. Zhu, H. Zheng, C.M. Ko et al., Light nuclei production in Pb+Pb collisions at $\sqrt{s_{NN}}$ = 2.76 TeV. Eur. Phys. J. A **54**, 175 (2018). https://doi.org/10.1140/epja/i2018-12610-7
26. W. Zhao, C. Shen, C.M. Ko et al., Beam-energy dependence of the production of light nuclei in Au + Au collisions. Phys. Rev. C **102**, 044912 (2020). https://doi.org/10.1103/PhysRevC.102.044912
27. R.Q. Wang, F.L. Shao, J. Song, Momentum dependence of light nuclei production in $p-p$, $p-Pb$, and Pb-Pb collisions at energies available at the CERN Large Hadron Collider. Phys. Rev. C **103**, 064908 (2021). https://doi.org/10.1103/PhysRevC.103.064908
28. Z.J. Dong, Q.Y. Wang, G. Chen et al., Energy dependence of light (anti)nuclei and (anti)hypertriton production in the Au-Au collision from $\sqrt{s_{NN}}$ = 11.5 to 5020 GeV. Eur. Phys. J. A **54**, 144 (2018). https://doi.org/10.1140/epja/i2018-12580-8
29. H. Liu, D. Zhang, S. He et al., Light nuclei production in Au+Au collisions at $\sqrt{s_{\rm NN}}$ = 5–200 GeV from JAM model. Phys. Lett. B **805**, 135452 (2020). https://doi.org/10.1016/j.physletb.2020.135452
30. X.G. Deng, Y.G. Ma, Light nuclei production in Au + Au collisions at $\sqrt{s_{\rm NN}}$ = 7.7–80 GeV from UrQMD model. Phys. Lett. B **808**, 135668 (2020). https://doi.org/10.1016/j.physletb.2020.135668
31. K.J. Sun, R. Wang, C.M. Ko et al., Relativistic kinetic approach to light nuclei production in high-energy nuclear collisions. arXiv:2106.12742 [nucl-th]
32. D. Oliinychenko, L.G. Pang, H. Elfner et al., Microscopic study of deuteron production in Pb–Pb collisions at $\sqrt{s}$ = 2.76 TeV via hydrodynamics and a hadronic afterburner. Phys. Rev. C **99**, 044907 (2019). https://doi.org/10.1103/PhysRevC.99.044907
33. J. Staudenmaier, D. Oliinychenko, J.M. Torres-Rincon et al., Deuteron production in relativistic heavy ion collisions via stochastic multiparticle reactions. Phys. Rev. C **104**, 034908 (2021). https://doi.org/10.1103/PhysRevC.104.034908

34. F. Retiere, M.A. Lisa, Observable implications of geometrical and dynamical aspects of freeze out in heavy ion collisions. Phys. Rev. C **70**, 044907 (2004). https://doi.org/10.1103/PhysRevC.70.044907
35. C.Y. Wong, G. Wilk, Tsallis fits to p_{T} spectra for pp collisions at LHC. Acta Phys. Polon. B **43**, 2047 (2012). https://doi.org/10.5506/APhysPolB.43.2047
36. C.Y. Wong, G. Wilk, Tsallis fits to p_T spectra and multiple hard scattering in pp collisions at the LHC. Phys. Rev. D **87**, 114007 (2013). https://doi.org/10.1103/PhysRevD.87.114007
37. A. Khuntia, S. Tripathy, R. Sahoo et al., Multiplicity dependence of non-extensive parameters for strange and multi-strange particles in proton-proton collisions at $\sqrt{s} = 7$ TeV at the LHC. Eur. Phys. J. A **53**, 103 (2017). https://doi.org/10.1140/epja/i2017-12291-8
38. H. Zheng, L. Zhu, A. Bonasera, Systematic analysis of hadron spectra in p+p collisions using Tsallis distributions. Phys. Rev. D **92**, 074009 (2015). https://doi.org/10.1103/PhysRevD.92.074009
39. H. Zheng, L. Zhu, Can Tsallis distribution fit all the particle spectra produced at RHIC and LHC? Adv. High Energy Phys. **2015**, 180491 (2015). https://doi.org/10.1155/2015/180491
40. H. Zheng, L. Zhu, Comparing the Tsallis distribution with and without thermodynamical description in $p + p$ collisions. Adv. High Energy Phys. **2016**, 9632126 (2016). https://doi.org/10.1155/2016/9632126
41. X. Yin, L. Zhu, H. Zheng, A new two-component model for hadron production in heavy-ion collisions. Adv. High Energy Phys. **2017**, 6708581 (2017). https://doi.org/10.1155/2017/6708581
42. H. Zheng, X. Zhu, L. Zhu et al., Systematic investigation of the particle spectra in heavy-ion collisions at the Large Hadron Collider. Mod. Phys. Lett. A **35**, 2050177 (2020). https://doi.org/10.1142/S0217732320501771
43. L. Zhu, H. Zheng, R. Kong, Centrality and transverse momentum dependencies of hadrons in Pb+Pb collisions at $\sqrt{s_{\mathrm{NN}}} = 5.02$ TeV and Xe+Xe collisions at $\sqrt{s_{\mathrm{NN}}} = 5.44$ TeV from a multi-phase transport model. Eur. Phys. J. A **55**, 205 (2019). https://doi.org/10.1140/epja/i2019-12903-3
44. The iEBE-MUSIC is a general-purpose numerical framework to simulate dynamical evolution of relativistic heavy-ion collisions event by event, which can be downloaded from [https://github.com/chunshen1987/iEBE- MUSIC]
45. W.M. Alberico, A. Lavagno, Non-extensive statistical effects in high-energy collisions. Eur. Phys. J. A **40**, 313 (2009). https://doi.org/10.1140/epja/i2009-10809-3